

Supplementary Information

Assessing the Internalization Pathways of Cr-Fe-Ni Nanoparticles in Native *Dittrichia viscosa* Naturally Exposed to Industrial Atmospheric Fallout

Bouchra Belhaj Abdallah^a, Irene Andreu^a, Viridiana Perez^a, and Byron D. Gates^{a*}

^a Department of Chemistry, Simon Fraser University, 8888 University Drive, Burnaby, British Columbia, V5A 1S6, Canada

Acknowledgements

We acknowledge Tunisian Steel Manufacturing Company El Fouladh. This project was sponsored by the PASRI program (Project for Supporting Research System and Innovation) funded by the European Union. This research was also funded in part by the Natural Sciences and Engineering Research Council (NSERC) of Canada (Discovery Grant no. RGPIN-2020-06522), and CMC Microsystems (MNT Grant nos. 3925 and 5342). This work made use of 4D LABS (www.4dlabs.ca) and the Centre for Soft Materials shared facilities at Simon Fraser University (SFU) supported by the Canada Foundation for Innovation (CFI), British Columbia Knowledge Development Fund (BCKDF), Western Economic Diversification Canada, and SFU.

Table of Contents

| | |
|---|-----|
| Section S1. Additional Data Associated with the Isolated Particulate Matter | S4 |
| Section S2. Analyses by X-ray Fluorescence (XRF) Spectroscopy..... | S11 |
| Section S3. Analyses by Inductively Coupled Plasma Mass Spectrometry (ICP-MS)..... | S12 |
| Section S4. Abbreviation and References..... | S19 |

Section S1. Additional Data Associated with the Isolated Particulate Matter.

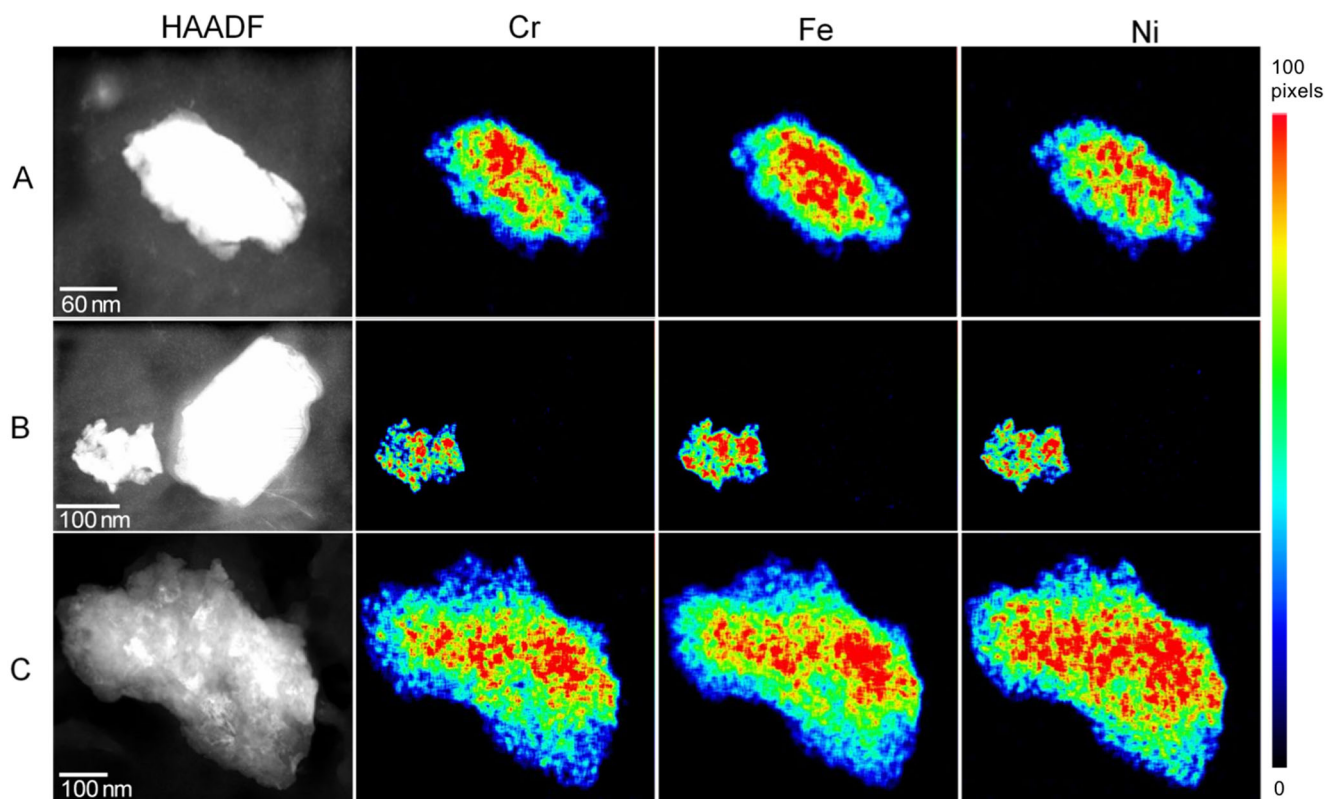


Figure S1 (part1). Additional scanning transmission electron microscopy (STEM) images obtained by high-angle annular dark-field (HAADF) techniques and elemental maps obtained by energy dispersive X-ray spectroscopy (EDS) of individual Cr-Fe-Ni nanoparticles (A-C) isolated from the leaves of *Dittrichia viscosa*. The vertical scale bar indicates the relative abundance of each element at each pixel within the EDS-based maps (i.e., red is associated with the highest concentration). These samples were obtained in proximity to an area associated with steel manufacturing activities.

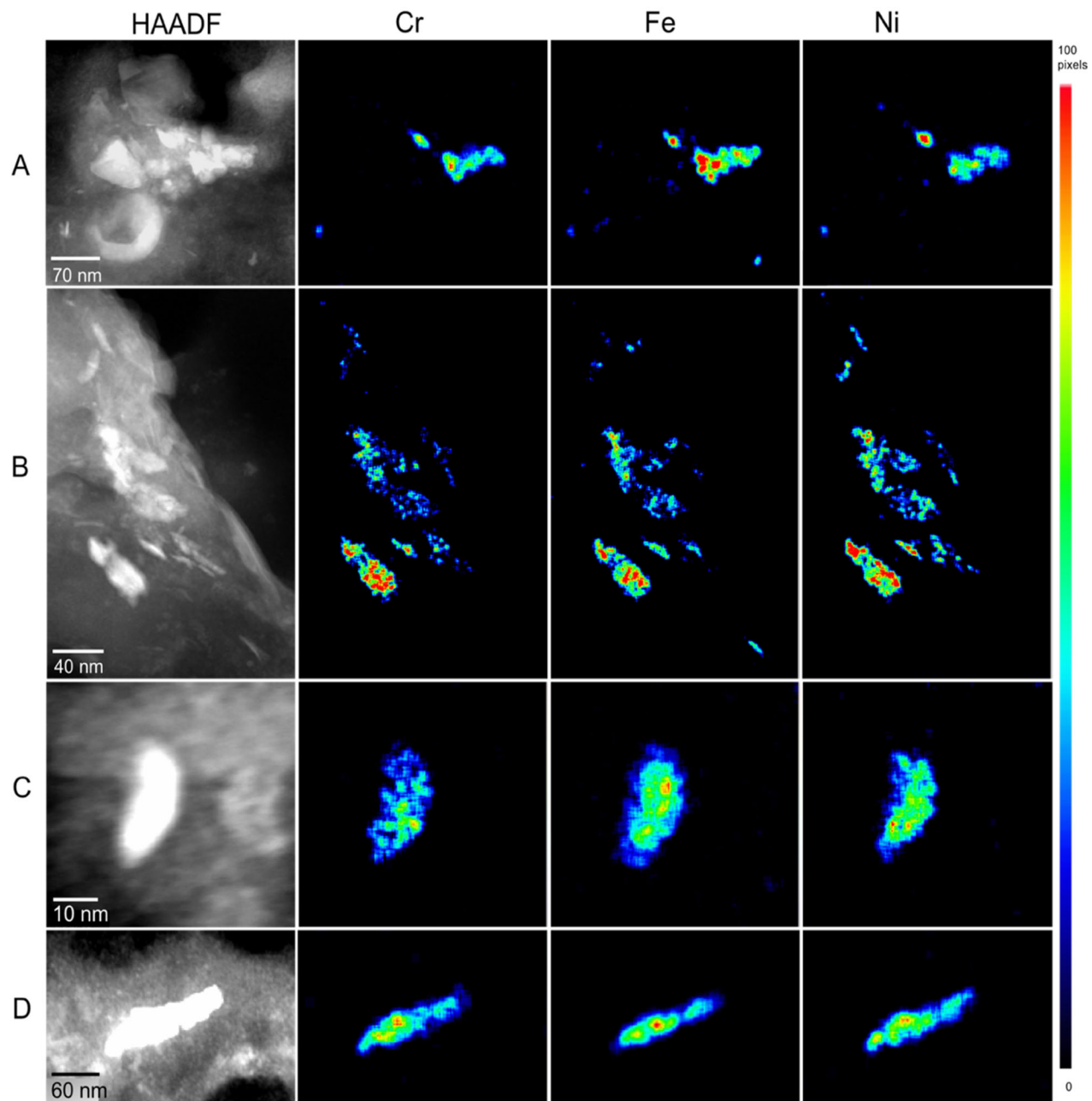


Figure S1 (part2). Additional STEM images obtained by HAADF techniques and elemental maps obtained by EDS for a series of Cr-Fe-Ni nanoparticles (A-D) isolated from the leaves of *Dittrichia viscosa*. These samples were obtained in proximity to an area associated with steel manufacturing activities.

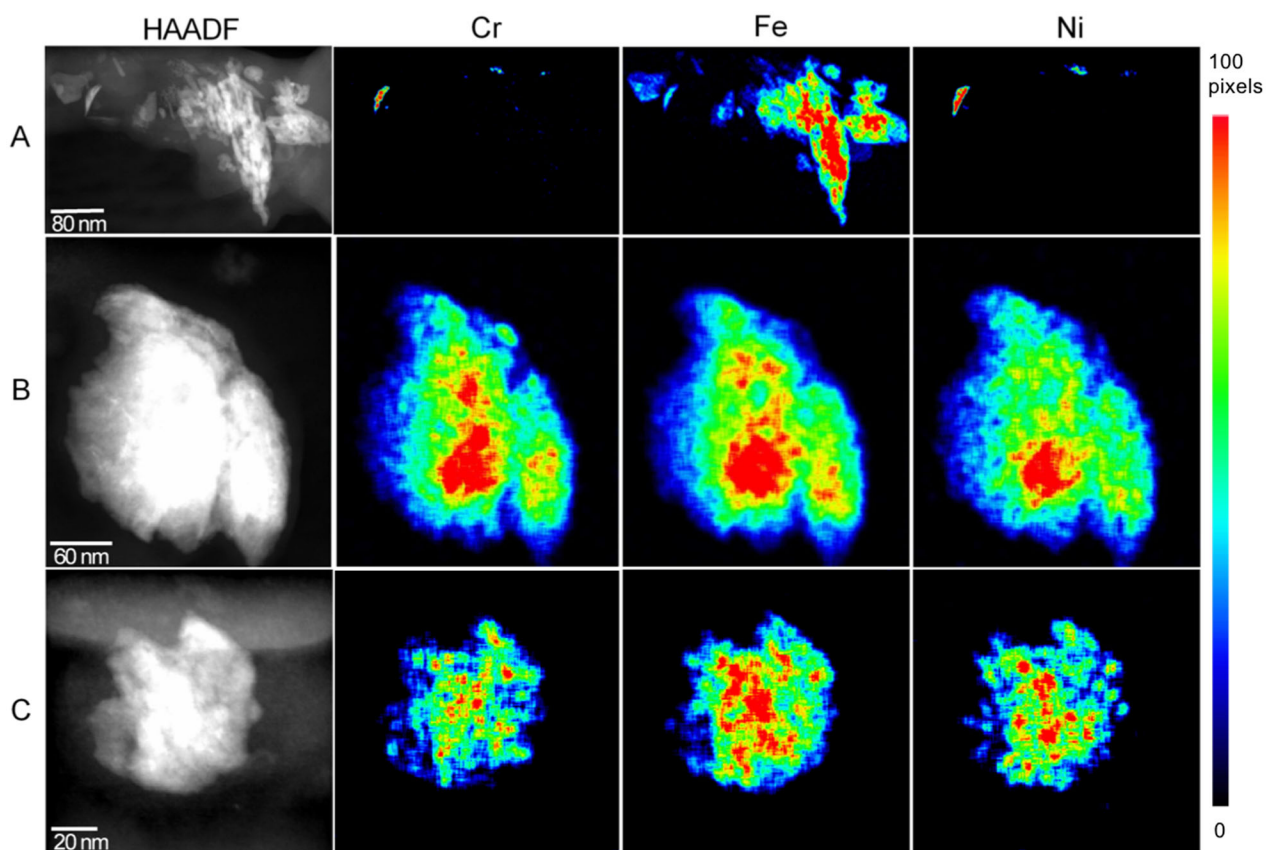


Figure S2 (part1). Additional STEM images obtained by HAADF techniques and EDS-based maps of Cr, Fe, and Ni species within nanoparticles (A-C) isolated from the stems of *Dittrichia viscosa*. These samples were obtained from an area in proximity to steel manufacturing activities.

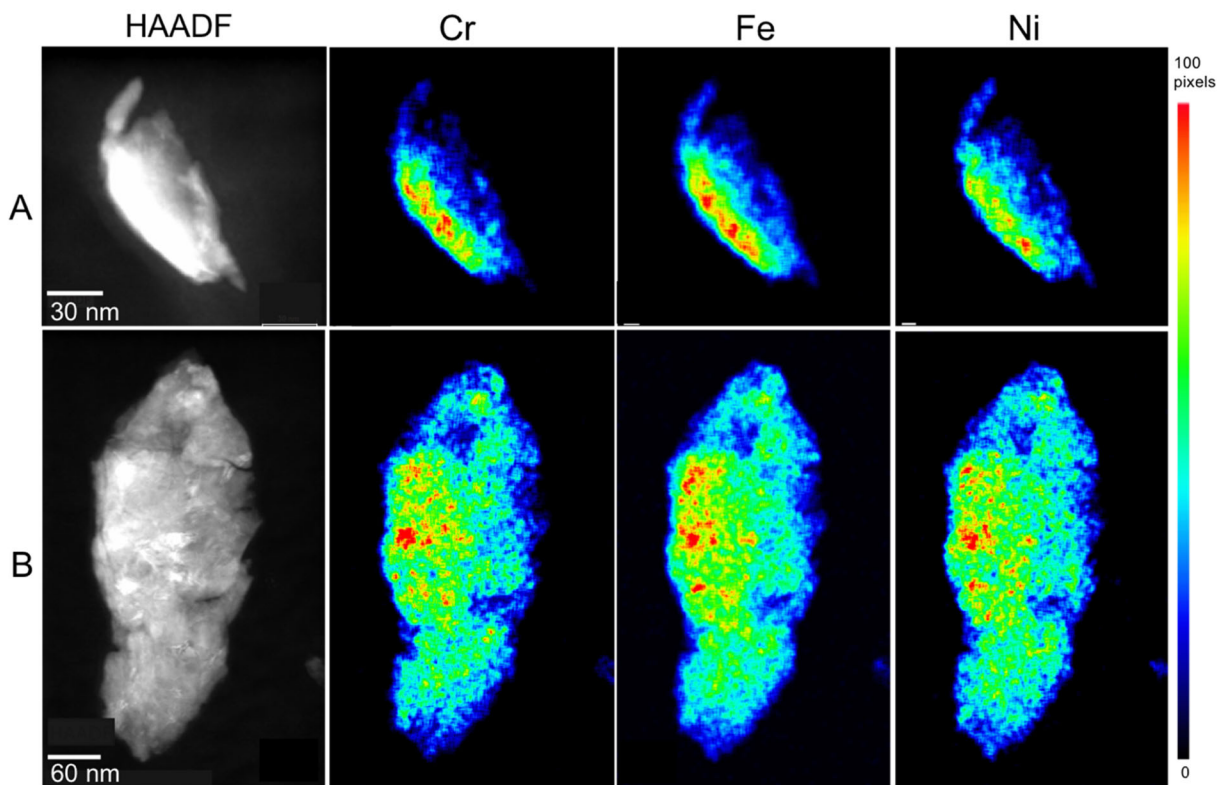


Figure S2 (part2). Additional STEM images obtained by HAADF techniques and EDS-based maps of Cr, Fe, and Ni within nanoparticles (A-B) isolated from the stems of *Dittrichia viscosa*. These samples were obtained from an area in proximity to steel manufacturing activities.

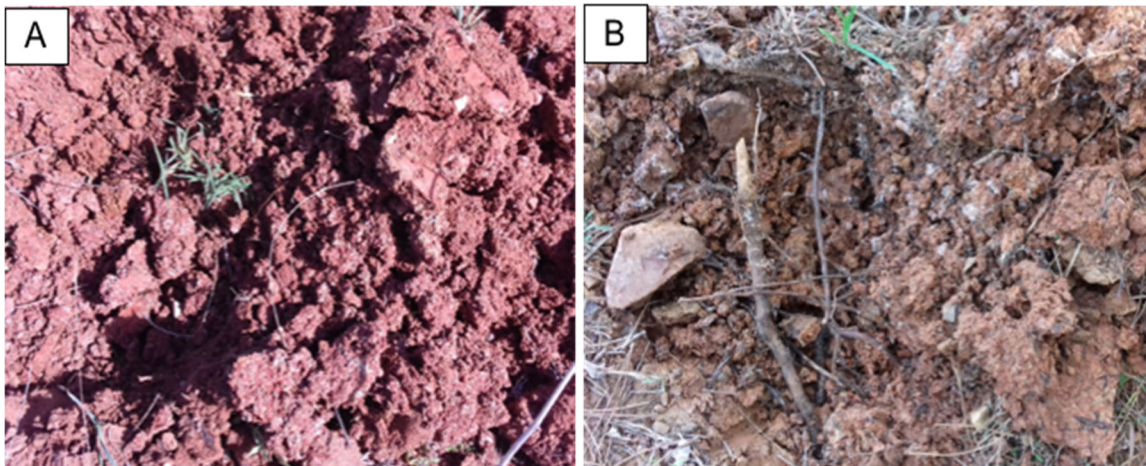


Figure S3. Photographs of (A) the rural rhizosphere with a metal content of $[\text{Ni}] < \text{LOD}$, $[\text{Fe}] = 23\,446 \text{ ppm} \pm 322$, $[\text{Cr}] = 86 \pm 5 \text{ ppm}$, and (B) the industrial rhizosphere where metal content was $[\text{Ni}] = 127 \pm 35 \text{ ppm}$, $[\text{Fe}] = 150\,683 \pm 35\,171 \text{ ppm}$, and $[\text{Cr}] = 300 \pm 92 \text{ ppm}$.

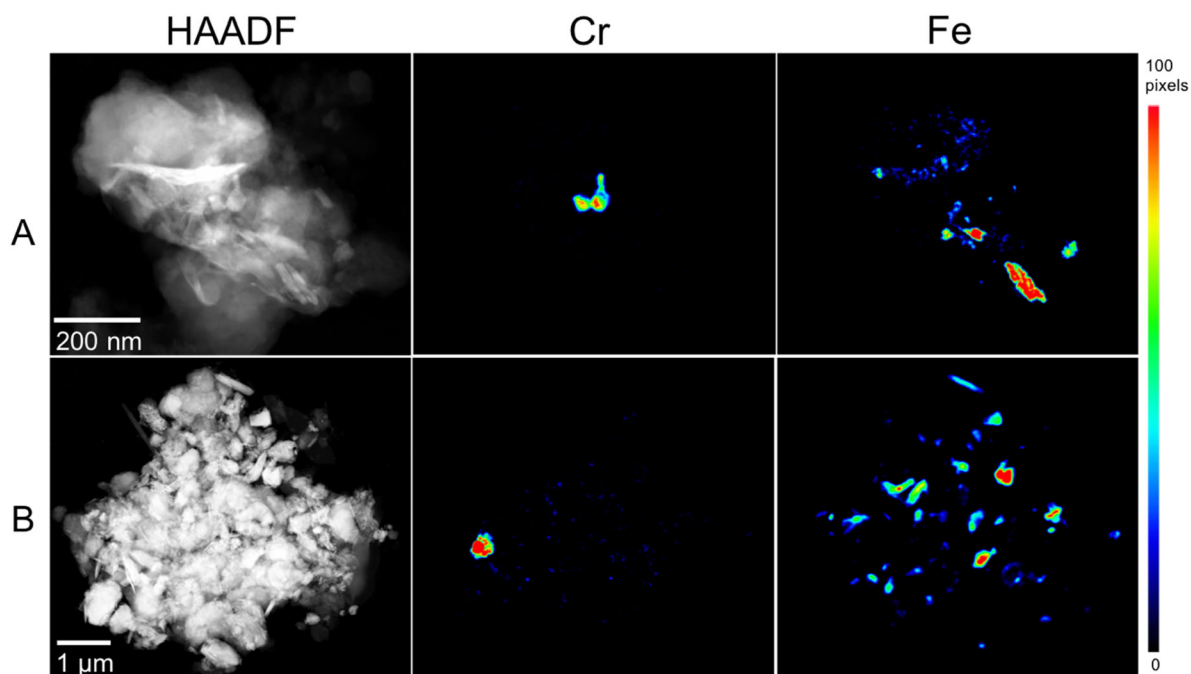


Figure S4. Images obtained by STEM-HAADF techniques and EDS-based mapping of individual Cr and Fe particulate matter isolated from (A) the leaves and (B) the rhizosphere of *Dittrichia viscosa*. Samples were collected from a region near steel manufacturing activities.

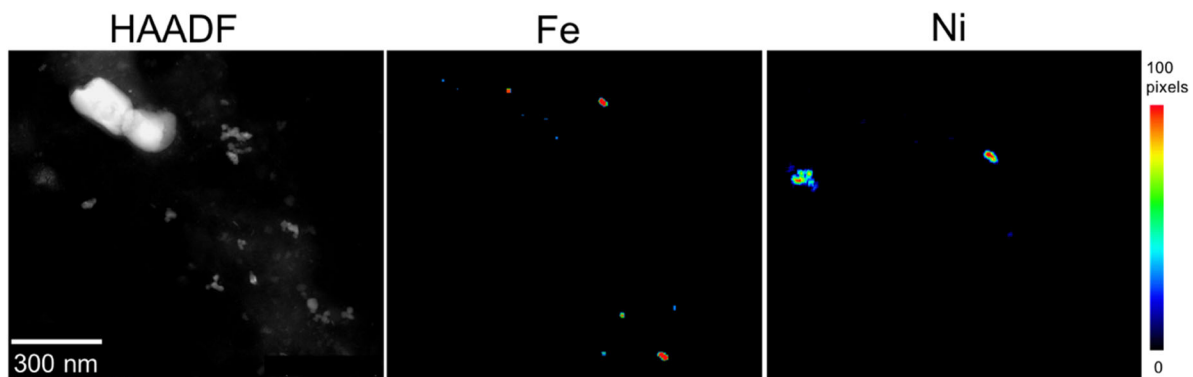


Figure S5. Additional images obtained by STEM-HAADF techniques and EDS-based mapping of individual Fe and Ni particulate matter isolated from the roots of *Dittrichia viscosa*. This sample was collected in proximity to an area associated with steel manufacturing.

Section S2. Analyses by X-ray Fluorescence (XRF) Spectroscopy

Table S1. Assessment of significant differences in the Cr, Fe, and Ni content as determined by XRF spectroscopy for each plant organ and rhizosphere when comparing samples obtained near an industrial site to those samples obtained from a rural area.

| plant organ and rhizosphere → | rhizospheres | roots | stems | leaves |
|--------------------------------------|---------------------|---------------|--------------|---------------|
| <i>P</i> value for Cr content | 0.008* | 0.0649 | 0.1032 | 0.0495* |
| <i>P</i> value for Fe content | 0.0002* | $< 10^{-5}$ * | 0.6824 | 0.0039* |
| <i>P</i> value for Ni content | 0.0027* | 0.8145 | 0.0208* | 0.9372 |

**P* values indicate the reported significance (tested by lm.nb) for the content of Cr, Fe, and Ni in each plant organ and rhizosphere collected from the industrial and rural area.

Section S3. Analyses by Inductively Coupled Plasma Mass Spectrometry (ICP-MS)

3.1. Experimental Methods for the ICP-MS Analyses

The same filters measured by XRF were further inspected for their Cr, Fe, and Ni content using inductively coupled plasma mass spectrometry (ICP-MS) as a semi-quantitative assessment. Special care was taken for cleaning the sample preparation area and the tools used during both the cutting of the filters and of the digestion of the samples. Filters containing the solids isolated from each plant organ and soil sample were cut into two equal pieces. Since ICP-MS is a destructive technique, only one section of each filter was initially digested for analysis by ICP-MS. Half of each of the filters were placed into separate, clean glass scintillation vials. Each of these sections of filter were digested with a 2 mL solution of concentrated nitric acid (Sigma Aldrich, HNO₃, 60% purity) for 2 h at 65°C. *Caution: Take appropriate precautions when handling nitric acid as it is corrosive.* A 1 mL aliquot of each acid digestion was diluted 50 times with ultrapure water (18 MΩ·cm water) to reach a final nitric acid concentration of 2% v/v, suitable for analysis on the ICP-MS instrument. Following this dilution, the samples were each filtered through polytetrafluoroethylene (PTFE) filters with a nominal pore size of 25 μm, and analyzed by ICP-MS using a Thermo Fisher Scientific iCAP Q. A survey mode was used to analyze all of the elements present in each of the samples. This survey scan enabled us to assess the relative changes in elemental composition of the control samples, the rural and industrial plant specimens, and within the different plant organs. Absolute concentrations of each element were not obtained in this study for a few reasons, including the limitations in our ability to accurately correlate the amount of each element to the total mass of each plant organ or soil sample due to material losses during the various stages required for isolating the nanoparticles. During extraction of the nanomaterials, the corresponding rhizospheres of these plant specimens are also likely to contain an additional fraction of nanomaterials that were not isolated in these

procedures. The solutions obtained during the isolation of the nanomaterials were decanted to remove large debris, and only 2 mL of each supernatant was filtered to obtain the isolated fractions of each sample. Additionally, there might be some fraction of nanomaterials that were not released or digested from the filters during their work-up for ICP-MS analysis; optimizing this sample digestion was beyond the scope of this study. Although not all of the isolated particulates were analyzed by the ICP-MS techniques, these analyses do yield a semi-quantitative assessment of the fractions of each element present in the sample and support the quantitative analyses by XRF.

A series of pristine filters were prepared and processed in the same manner as the treatment given to each sample, but without the introduction of the solids isolated from the plant organs or rhizospheres. This process created a series of “blank” filters that served as additional control samples, such as to monitor for the introduction of contamination from the method (e.g., from the reagents and/or filters used in the process).

3.2. Results and Further Discussion from the ICP-MS Analyses

The ICP-MS analyses were used as a complementary analysis to the use of XRF for studying the solid fractions collected by extraction and filtration processes from each of the plant specimens and their rhizospheres. A survey scan performed by ICP-MS was utilized for a semi-quantitative analysis of the presence of the heavy metals of interest. This analysis was used as an additional confirmation of the presence of the heavy metals of interest within the plants and their corresponding rhizospheres (Figure S6). The metal content on three separate filters obtained from each plant organ, as well as three samples obtained from the corresponding rhizosphere of each plant specimen were each analyzed by ICP-MS.

The plant specimens and rhizospheres obtained in proximity to the steel manufacturing site had a similar trend as the specimens collected in a rural area when analyzing for the Cr, Fe, and Ni content. This data was confirmed statistically. In general, there were no significant differences observed in the Fe, Cr, and Ni content of the plant organs and the rhizospheres of the plants collected near the industrial site and those harvested from the rural site (Table S2). A significant difference was observed for the Fe at the rhizosphere level between these two sites. Note that the ICP-MS equipment we had access to measures the concentrations of dissolved elemental species in an acidic solution, but was not able to measure the concentration of metals present as suspended micrometer sized or nanometer sized particles. There could, as a result, be contributions from both particulate matter and ionic species present in these analyses.

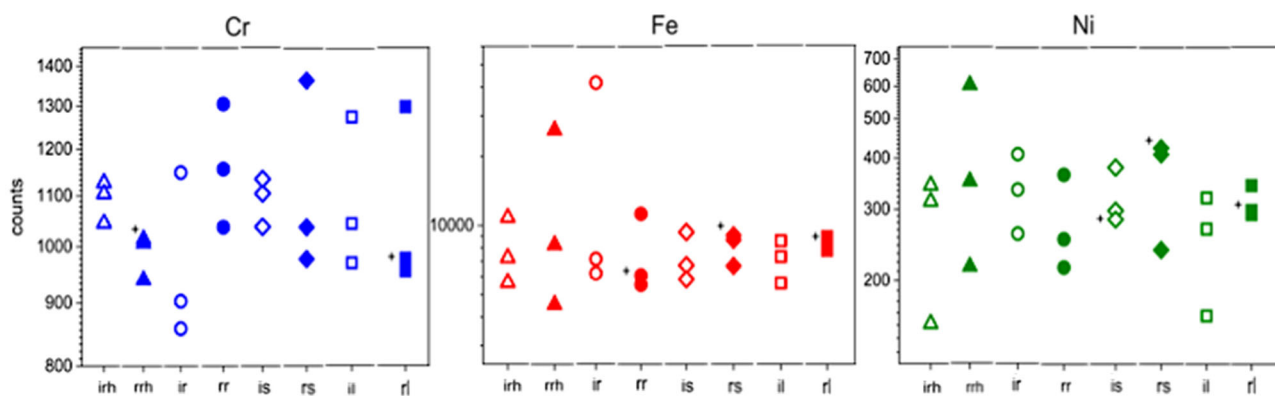


Figure S6. Results from the inductively coupled plasma mass spectrometry (ICP-MS) analyses of Fe, Cr, and Ni found within each plant organ and rhizosphere of *Dittrichia viscosa*, which were harvested from the industrial and rural regions of interest. Three distinct replicate samples (n=3) were used for each set of measurements. The + indicates an overlap of replicate measurements. (Primary symbols: i – industrial site and r – rural site; and secondary symbols: rh – rhizosphere; r – roots; s – stems; and l – leaves).

Iron was present in higher amounts relative to the other metals of interest in all the plant specimens and plant organs. The root organ of the plant specimens collected in proximity to the steel manufacturing site and in the rural area had higher Fe counts than the other plant organs associated with these samples. The stems and leaves of specimens collected from both the industrial and rural regions exhibited a similar total Fe content. These results suggest that the plants were translocating similar amounts of iron from either the soil through root uptake or from the leaves through foliar uptake. The availability of a wide range of Fe species that can be present in the environment may enhance their uptake. Speciation and transport processes are largely dictated by the pH of the soil.¹ These results from the ICP-MS analyses agree with what has been observed by XRF, which further suggests that the root-rhizosphere interface was not a barrier to iron uptake.

Table S2. Assessing the statistical significance between the different Cr, Fe, and Ni content of each plant organ and rhizosphere as determined by ICP-MS when comparing samples obtained near the industrial site and those from a rural area.

| plant organ and rhizosphere → | rhizospheres | roots | stems | leaves |
|--------------------------------------|---------------------|--------------|--------------|---------------|
| <i>P</i> value for Cr content | 0.0375* | 0.1748 | 0.7927 | 0.8968 |
| <i>P</i> value for Fe content | 0.5006 | 0.4155 | 0.5633 | 0.2749 |
| <i>P</i> value for Ni content | 0.4025 | 0.4096 | 0.6074 | 0.2889 |

**P* values indicate the reported significance (tested by lm.nb) of Cr, Fe, and Ni content in each plant organ and rhizosphere collected from the industrial and rural area.

The Cr content within the aerial organs was larger than in the roots. In addition, the rhizospheres from the plant specimens sampled near to the steel manufacturing also had higher Cr counts relative to that in the rhizosphere of the plants in the rural region. Similar counts for Cr were

observed between those found in the stems and those in the leaves. It is possible that the chromium species in the rhizosphere, stems, and leaves were present as particulate matter containing Cr-Fe-Ni.

The data from the ICP-MS survey scans (Figure S6) indicate that the Ni was sequestered in a similar manner among the plant organs of *Dittrichia viscosa* sampled from the rural area and the plant species that were collected near the area of steel manufacturing. The availability of Ni in the rhizosphere of the plants growing in the rural area could increase its accessibility to the corresponding plant organs via relatively efficient translocation pathways. It is possible that the Ni species are transported as either coordination complexes or particulate matter, which could also be transported through the air. If airborne fractions are a dominant form of transport, the aerial plant organs could have more Ni content in comparison to the shoot organs from the plant when in proximity to industrial activities. Compared to the rural area, the relatively low count of Ni in the leaves of the plant species collected near to the industrial activities may be due to the heterogeneous distribution of the isolated solid particles collected on the surfaces of the filter. A similar Cr, Fe, and Ni content was confirmed through a statistical analysis of the results and was found to also be consistent between the plant specimens collected from either type of site (industrial or rural). It is likely that these results do not correlate with the results of the XRF analyses due to an incomplete digestion of the samples in preparation for the analysis by ICP-MS techniques. If only a small fraction of the total particulate matter isolated from the rhizospheres and plant organs was digested, the quantification by ICP-MS would be inaccurate as a result.² This might be due to Cr-Fe-Ni particles that were not sufficiently digested when using nitric acid for sample preparation in contrast to when microwave digestion methods are used along with a mixture of acids such as hydrochloric, hydrofluoric, and/or nitric acid (e.g., HCl mixed with HNO₃ or HF mixed with HNO₃).³ It has been reported that nitric acid alone can be less effective towards dissolution of some metals than when using mixed acids for the

digestion of particulate matter.² For example, iron oxide based minerals are not efficiently attacked with nitric acid alone to liberate any other metals associated with these minerals (e.g., metals incorporated as dopants or inclusions). This could extend to the inability of the methodology to effectively release Cr and Ni within the Cr-Fe-Ni particulate matter identified through the TEM analyses. In addition, the silica and alumina present within the matrices of the isolated nanomaterials could also occlude the detection of metal species by ICP-MS. Hydrofluoric acid is often required to release metal content that would otherwise be contained within a silica or alumina based matrix. Only nitric acid based digestions were permitted for use on the ICP-MS system we had access to in a shared facility, which was not equipped to handle other acids such as hydrofluoric acid. In addition, as mentioned above, this system was not equipped to accurately detect the relatively small particulate matter present in the samples that might have not been thoroughly digested or retained by the filtration step prior to ICP-MS analysis. Thus, these ICP-MS based results are likely to be under representing the content of the isolated samples. In the future studies it is recommended to use a system that can handle a wider range of acid digestions and/or a system that can adequately analyze nanoparticle fractions suspended within the sample matrix.

The abundance of Cr-Fe-Ni containing particles in the stems and leaves of the plant specimens collected in proximity to the steel manufacturing activities suggests the uptake of airborne Cr-Fe-Ni particulate matter from processes such as foliar uptake.^{4,5} The internalized Cr-Fe-Ni nanoparticles could be subsequently translocated throughout the plants, including to the roots, through the phloem sap.^{4,6-9} Alternatively, these nanoparticles could have been biosynthesized by the plant tissues from smaller individual Fe, Cr, and Ni nanoparticles from atmospheric deposition or uptake through the stomata of the leaves. Separate Cr, Fe, and Ni containing nanoparticles could be first assimilated by the aerial parts, and/or the root organs of the plant species, and subsequently transformed into the

irregularly shaped Cr-Fe-Ni nanoparticles observed within the plant tissues. Individual nanoparticles of Cr, Fe, and Ni or nanoparticles of Cr-Fe-Ni can each be present in the exhaust following combustion processes, smelting activities and mechanical processing during steel manufacturing.

Section S4. Abbreviations and References

Abbreviations

| | |
|--------|--|
| EDS | Energy Dispersive X-ray Spectroscopy |
| HAADF | High-Angle Annular Dark-Field |
| ICP-MS | Inductively Coupled Plasma Mass Spectrometry |
| SEM | Scanning Electron Microscopy |
| STEM | Scanning Transmission Electron Microscopy |
| TEM | Transmission Electron Microscopy |
| XRF | X-ray Fluorescence |

References

- (1) J. Morrissey, M.L. Guerinot, Iron Uptake and Transport in Plants: The Good, the Bad, and the Ionome, *Chem. Rev.*, 2009, **109**, 4553–4567.
- (2) S. Lamine, G.P. Petropoulos, P.A. Brewer, N. Bachari, P.K. Srivastava, K. Manevski, C. Kalaitzidis, M.G. Macklin, Heavy Metal Soil Contamination Detection Using Combined Geochemistry and Field Spectroradiometry in the United Kingdom, *Sensors*, 2019, **19**, 1–16.
- (3) D. Remeteiová, S. Ružičková, V. Micková, M. Martina Laubertová, R. Slezáková, EPA Evaluation of US EPA Method 3052 Microwave Acid Digestion for Quantification of Majority Metals in Waste Printed Circuit Boards, *Metals*, 2020, **10**, 1–12.

- (4) C. Larue, H. Castillo-Michel, S. Sobanska, N. Trcera, S. Sorieul, L. Cécillon, L. Ouerdane, S. Legros, G. Sarret, Fate of Pristine TiO₂ Nanoparticles and Aged Paint-Containing TiO₂ Nanoparticles in Lettuce Crop After Foliar Exposure, *J. Hazard. Mater.*, 2014, **273**, 17–26.
- (5) C. Uhlig, O. Juntila, Airborne Heavy Metal Pollution and its Effects on Foliar Elemental Composition of *Empetrum Hermaphroditum* and *Vaccinium Myrtillus* in Sør-Varanger, Northern Norway, *Environ. Pollut.*, 2001, 114, 461–469.
- (6) N. Ha, E. Seo, S Kim, S.J. Lee, Adsorption of Nanoparticles Suspended in a Drop on a Leaf Surface of *Perilla Frutescens* and Their Infiltration Through Stomatal Pathway, *Sci. Rep.*, 2021, **11**, 1–13.
- (7) M.R. Khan, V. Adam, T. Fatima Rizvi, B. Zhang, F. Ahamad, I. Josko, Y. Zhu, M. Yang, C. Mao, Nanoparticle-Plant Interactions: A Two-Way Traffic, *Small*, 2019, **15**, 1–37.
- (8) F. Schwab, G. Zhai, M. Kern, A. Turner, J.L. Schnoor, M.R. Wiesner, Barriers, Pathways and Processes for Uptake, Translocation and Accumulation of Nanomaterials in Plants, *Nanotoxicology*, 2016, **10**, 257–78.
- (9) Y. Su, V. Ashworth, C. Kim, A.S. Adeleye, P. Rolshausen, C. Roper, J. Jason White, D. Jassby, Delivery, Uptake, Fate, and Transport of Engineered Nanoparticles in Plants: A Critical Review and Data Analysis, *Environ. Sci. Nano*, 2019, **6**, 2311–2331.